

DIFFender: Diffusion-Based Adversarial Defense against Patch Attacks

Caixin Kang¹, Yinpeng Dong², Zhengyi Wang², Shouwei Ruan¹, Yubo Chen³,
Hang Su², Xingxing Wei^{1*}

¹ Beihang University ² Tsinghua University ³ Beijing Institute of Technology
{caixinkang, shouweiruan, xxwei}@buaa.edu.cn;
{dongyinpeng, wang-zy21, suhangss}@tsinghua.edu.cn;

Abstract

Adversarial attacks, particularly patch attacks, pose significant threats to the robustness and reliability of deep learning models. Developing reliable defenses against patch attacks is crucial for real-world applications, yet current research in this area is unsatisfactory. In this paper, we propose *DIFFender*, a novel defense method that leverages a text-guided diffusion model to defend against adversarial patches. *DIFFender* includes two main stages: patch localization and patch restoration. In the localization stage, we find and exploit an intriguing property of the diffusion model to precisely identify the locations of adversarial patches. In the restoration stage, we employ the diffusion model to reconstruct the adversarial regions in the images while preserving the integrity of the visual content. Thanks to the former finding, these two stages can be simultaneously guided by a unified diffusion model. Thus, we can utilize the close interaction between them to improve the whole defense performance. Moreover, we propose a few-shot prompt-tuning algorithm to fine-tune the diffusion model, enabling the pre-trained diffusion model to adapt to the defense task easily. We conduct extensive experiments on image classification, face recognition, and further in the physical world, demonstrating that our proposed method exhibits superior robustness under strong adaptive attacks and generalizes well across various scenarios, diverse classifiers, and multiple patch attack methods.

1. Introduction

Deep neural networks are vulnerable to adversarial examples [9, 29], in which imperceptible perturbations are intentionally added to natural examples, leading to incorrect predictions with high confidence of the model. Most adversarial attacks and defenses are devoted to studying the ℓ_p -norm threat models [3, 6, 9, 21], which assume that the adversarial perturbations are restricted by the ℓ_p norm to

be imperceptible. However, the classic ℓ_p perturbations require modification of every pixel of the images, which is typically not practical in the physical world. On the other hand, adversarial patch attacks [2, 17, 18, 33], which usually apply perturbations to a localized region of the objects, are more physically realizable. Adversarial patch attacks pose significant threats to real-world applications, such as face recognition [27, 37], autonomous driving [16, 44].

Although many adversarial defenses against patch attacks have been proposed in the past years, the defense performance is not satisfactory, which cannot meet the demands of the safety and reliability of real-world applications. Some methods employ adversarial training [25, 35] and certified defenses [4, 10], which are only effective against specific attacks but generalize poorly to other forms of patch attacks in the real world [24]. Another category of patch defense is based on pre-processing techniques [11, 20, 23, 40], which usually destroy the patterns of adversarial patches by image completion or smoothing. However, these methods can hardly restore the images with high fidelity, leading to visual artifacts of the reconstructed images that impact recognition. They can also be evaded by stronger adaptive attacks due to gradient obfuscation [1].

Recently, diffusion models [14, 28] have emerged as a powerful family of generative models, and have been successfully applied to improving adversarial robustness by purifying the input data [24, 32, 36]. By diffusing the adversarial examples with Gaussian noises and recovering the original inputs through the reverse denoising process of diffusion models, the downstream classifiers can correctly recognize the denoised images with high robustness. Our initial intuition is to explore whether diffusion purification can defend against patch attacks. However, we observe that the patch region in the adversarial image can hardly be denoised towards the clean image, while the output also differs from the raw patch. This suggests the potential to adopt diffusion models to detect the patch region, as shown in Fig. 1.

Based on the observation, we propose **DIFFender**, a novel defense method against adversarial patch attacks with

*Corresponding Authors.

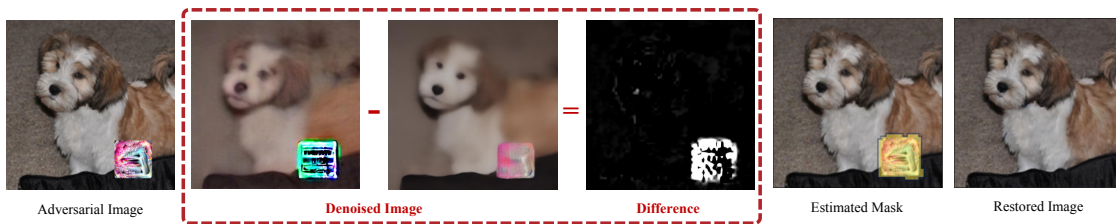


Figure 1. The intriguing property of the diffusion model. We perform a diffusion model multiple times on the given adversarial image, and find the differences between any two various denoised images are pronounced within the adversarial patch regions, which can be used to estimate the mask for this adversarial patch.

pre-trained diffusion models. DIFFender localizes the region of the adversarial patch by comparing the differences between various denoised images and then recovers the identified patch region in the image while preserving the integrity of the underlying content. Importantly, these two stages are carefully guided by a unified diffusion model, thus we can utilize the close interaction between them to improve the whole defense performance (i.e., an accurate localization will promote the following restoration, and a perfect restoration will help evaluate the performance of localization step in return). Specifically, we incorporate a text-guided diffusion model such that DIFFender can localize and recover the adversarial patches more accurately with textual prompts. Moreover, we design a few-shot prompt-tuning algorithm to facilitate simple and efficient tuning, enabling the pre-trained diffusion model to easily adapt to the adversarial defense task for improved robustness. The pipeline of DIFFender is illustrated in Fig. 2.

In summary, our contributions are as follows:

- We discover the intriguing property of the diffusion model, that is, disparities exist in the alteration magnitude between the adversarial patch and background regions during the diffusion denoising process, where the difference between any two various denoised images can be further used to identify the adversarial patch.
- Arising from the keen observations, we utilize a unified diffusion model throughout the entire process to localize and restore adversarial patches. Furthermore, we design an effective prompt-tuning algorithm that empowers the diffusion model to seamlessly adapt to the defense task. To the best of our knowledge, this is the first work to defend against patch attacks based on the diffusion model.
- We conduct extensive experiments on image classification, face recognition, and further in the physical world, demonstrating that DIFFender exhibits superior robustness under adversarial patch attacks. The results indicate that DIFFender can also generalize well to various scenarios, diverse classifiers, and multiple attack methods.

2. Related work

Adversarial attacks. Deep neural networks (DNNs) can be misled to produce erroneous outputs by introducing small perturbations to input examples. Most adversarial attacks [6, 9, 21, 22] typically induce misclassification or detection

errors by adding small perturbations to the pixels of input examples. However, while these methods can effectively generate adversarial examples in the digital world, they lack practicality in the real world. On the other hand, adversarial patch attacks aim to deceive models by applying a pattern or a sticker to a localized region of the object, which are more realizable in the physical world [2, 17, 18, 33, 42].

Adversarial defenses. With the development of attacks, various defense methods have been proposed. However, most existing defenses primarily focus on global perturbations with ℓ_p norm constraints, including former diffusion-based defenses [24, 32, 36], and defenses against patch attacks have not been extensively studied. Despite the effectiveness of adversarial training [25, 35] and certified defenses [4, 10] against specific attacks, they have limited generalization to other patch attacks.

Therefore, most studies focus on pre-processing defenses. Digital Watermarking [11] utilizes saliency maps to detect adversarial regions and employs erosion operations to remove small holes. Local Gradient Smoothing [23] performs gradient smoothing on regions with high gradient amplitudes, taking into account the high-frequency noise introduced by patch attacks. Feature Normalization and Clipping [40] involves gradient clipping operations on images to reduce informative class evidence based on knowledge of the network structure. Jedi [31] utilizes entropy to obtain masks. However, these methods can hardly reconstruct the original image and can be evaded by adaptive attacks [1]. In contrast, we propose to leverage pre-trained diffusion models to better localize and restore the adversarial patches.

3. Methodology

In this section, we first give the intriguing property of diffusion models to localizing patch regions, and then introduce the whole framework of our DIFFender.

3.1. Observation

DiffPure [24] is a recent method that utilizes diffusion models to remove the imperceptible perturbations on the images by input purification. It first adds Gaussian noise with a noise ratio t^* to the adversarial image and then denoises the image with the backward process of diffusion models. We first examine whether DiffPure can be applied to defend against patch attacks. As illustrated in Fig. 3, DiffPure is ineffective against patch attacks. We utilize diffu-

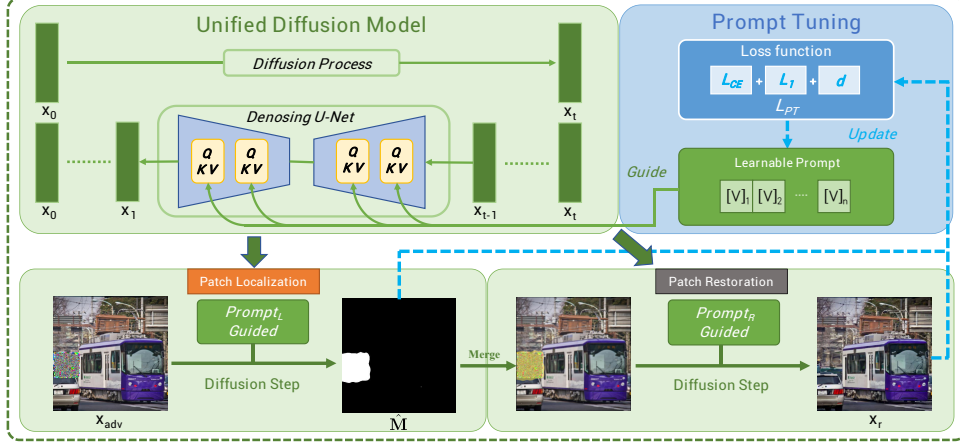


Figure 2. Pipeline of DIFFender. DIFFender leverages a unified diffusion model to jointly guide the localization and restoration of adversarial attacks, and combines a prompt-tuning module to facilitate efficient tuning.

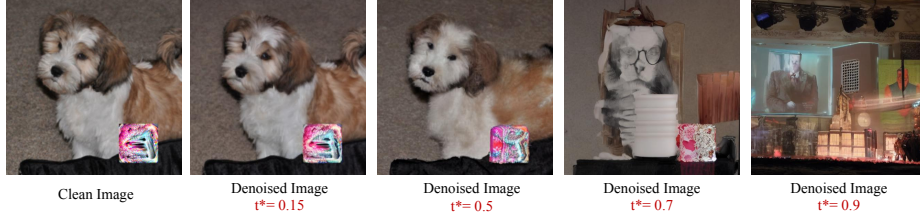


Figure 3. Restoration results denoised by diffusion model at noise ratios $t^* = 0.15/0.5/0.7/0.9$. The patch cannot be removed with small ratios (see $t^* = 0.15/0.5$), but the global structure gets lost with large ratios (see $t^* = 0.7/0.9$).

sion model to purify adversarial patches at different noise ratios t^* (parameterized within the range of 0 to 1), and find that it fails to eliminate the threat posed by adversarial patches while preserving the image semantics. This is due to the trade-off between purifying the adversarial perturbations (with a larger t^*) and preserving the image semantics (with a smaller t^*), making it impossible to find an appropriate noise ratio that can defend against adversarial patches.

Although the results indicate that DiffPure is not applicable to adversarial patches, we also find that when the noise ratio is about 0.5, the patch region in the adversarial image can hardly be denoised, but other regions outside the adversarial patch can be well-preserved. It indicates that we can calculate the difference between various denoised images to identify the region of adversarial patches. Several examples of this phenomenon are given in Fig. 4. The reason behind this phenomenon may be that adversarial patches are often meticulously crafted perturbations with a complexity far exceeding the noise present in real image datasets. Alternatively, it could be some meaningful sticker placed in an inappropriate location, signifying that the patch is out of context within the scenario. Diffusion models are trained to learn the probability distribution of real images, thus they struggle to fully adapt to the distribution of adversarial examples, leading to inaccurate estimations.

Due to the crucial observation, which can resolve the trade-off between purifying adversarial attacks and preserv-

ing image semantics when utilizing the diffusion model, we are now able to employ a single diffusion model, which first locates the patch attack and subsequently restores it.

3.2. DIFFender

Patch localization. DIFFender first performs accurate patch localization based on the above observation of the diffusion model. Given the adversarial image \mathbf{x}_{adv} , we first add Gaussian noise to create a noisy image \mathbf{x}_t with noise ratio 0.5. Next, we apply a text-guided diffusion model to obtain a denoised image \mathbf{x}_p from \mathbf{x}_t with a textual prompt $prompt_L$, and \mathbf{x}_e with empty text. We can estimate the mask region $\hat{\mathbf{M}}$ by taking the difference between the denoised images \mathbf{x}_p and \mathbf{x}_e . However, the diffusion model incurs a significant time cost due to the time steps T required. To address this issue, we directly predict the image \mathbf{x}_0 from the noisy image \mathbf{x}_t with only one step, which saves T times the processing time, based on the specific diffusion model.

Although the one-step predicted results often exhibit discrepancies and increased blurriness compared to the original image, the differences between one-step predictions still align with our observations. In practice, we perform one-step denoising twice, obtaining two results: \mathbf{x}_a , the one guided by $prompt_L$, and \mathbf{x}_b , the one guided by empty text to calculate the difference and binarize it, as:

$$\hat{\mathbf{M}} = \text{Binarize} \left(\frac{1}{m} \sum_{i=0}^m (\mathbf{x}_a^i - \mathbf{x}_b^i) \right), \quad (1)$$

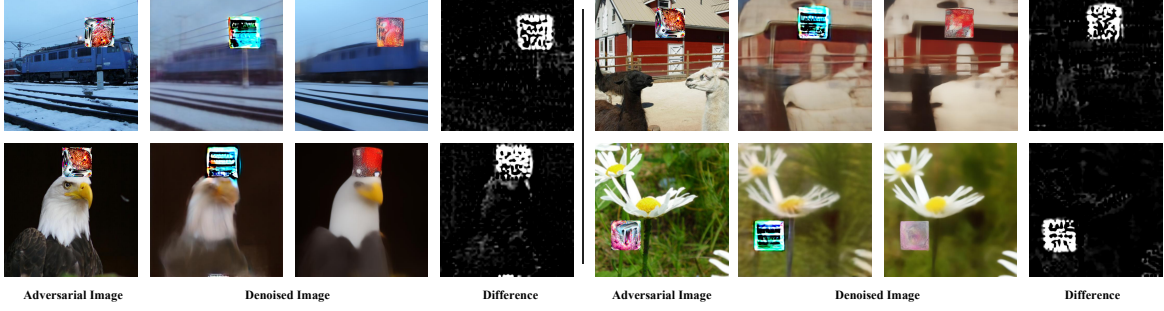


Figure 4. We test the difference results on 100 images from ImageNet and find that differences between any two various denoised images become more pronounced within the adversarial patch regions.

where we calculate the difference for m times (set to 3 in the experiments) to enhance the stability, eliminate randomness, and reduce the computational complexity. The $prompt_L$ can be hand-designed (e.g., “adversarial”) or automatically tuned as shown in Sec. 3.3.

Mask refining. As shown in Fig. 5, directly obtained averaged difference may sometimes result in minor inaccuracies. Therefore, we binarize the difference to gain the initial mask and then refine it by sequentially applying Gaussian smoothing and dilation operations, leading to a precise estimation of the patch region. The processed mask edges may slightly extend beyond the patch area, which helps maintain consistency in the patch restoration, thereby enhancing the overall performance of the defense pipeline.

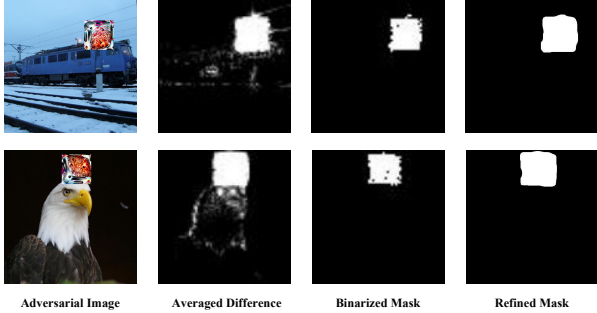


Figure 5. The estimated difference are binarized and applied Gaussian smoothing and dilation operations to gain the refined mask.

Patch restoration. After locating the patch region, DIFender then restores it to eliminate the adversarial effects, while also considering preserving the overall coherence and quality of the image. In particular, we combine the estimated mask \hat{M} and x_{adv} as inputs to the text-guided diffusion model with prompt $prompt_R$ to obtain a restored image x_r . We follow the inpainting pipeline in Stable Diffusion [26] to process the mask, where a UNet is used with an additional five input channels to incorporate the estimated mask \hat{M} . Similarly, $prompt_R$ can be manually set (e.g., “clean”) or automatically tuned.

To ensure the adversarial effect is removed in the images, the restoration performs the entire diffusion process, which

takes several times the processing time of the localization. However, the restoration is only invoked when attacks are detected, ensuring high efficiency (See Appendix B.1).

Unified defense model. The aforementioned two stages have been meticulously integrated into one unified diffusion model (e.g., stable diffusion), driven by our critical observations. This intentional fusion allows us to harness the tight interplay between these stages, thereby enhancing the defense mechanism. As a direct consequence of our insights, we also introduced the prompt-tuning module, which encompasses the joint optimization of the entire pipeline.

3.3. Prompt Tuning

Following the aforementioned pipeline, leveraging visual-language pre-training, DIFender is capable of efficiently performing zero-shot patch localization. While it is accurate in locating adversarial regions in most cases, subtle discrepancies in the segmented masks may occur in certain situations. Given that visual-language pretraining takes advantage of large-capacity text encoders to explore a vast semantic space [43], to facilitate the effective adaptation of learned representations into adversarial defense tasks, we introduce the algorithm of prompt tuning.

Learnable prompts. First, we replace the textual vocabulary with the learnable continuous vectors. Thus, $prompt_L$ and $prompt_R$ can be transformed into vectors as follows:

$$\begin{aligned} prompt_L &= [V_L]_1 [V_L]_2 \dots [V_L]_n; \\ prompt_R &= [V_R]_1 [V_R]_2 \dots [V_R]_n, \end{aligned} \quad (2)$$

where each $[V_S]_i$ or $[V_R]_i$ ($i \in \{1, \dots, n\}$) is a vector of the same dimensionality as word embeddings. n is a hyper-parameter that specifies the number of context tokens, we set $n = 16$ by default. The text content used to initialize $prompt_L$ and $prompt_R$ can be manually provided or randomly initialized.

Tuning process. After obtaining the learnable vectors, we design three loss functions for prompt tuning, which jointly optimize the vectors to capture the characteristics of the adversarial regions and improve the defense performance.

First, to accurately identify the adversarial regions for the localization module, we employ cross-entropy loss by comparing estimated mask $\hat{\mathbf{M}}$ with ground-truth mask \mathbf{M} .

$$L_{CE}(\mathbf{M}, \hat{\mathbf{M}}) = - \sum_{i=1}^d \mathbf{M}_i \log(\hat{\mathbf{M}}_i), \quad (3)$$

where i indicates the i -th element of the mask. Next, in the patch restoration module, our objective is to restore the mask region while eliminating the adversarial effect of the image. To ensure effective defense, we calculate the ℓ_1 distance between restored image \mathbf{x}_r and clean image \mathbf{x} as:

$$L_1(\mathbf{x}_r, \mathbf{x}) = |\mathbf{x}_r - \mathbf{x}|. \quad (4)$$

Lastly, to verify that the adversarial effects have been eliminated, we draw inspiration from [19] and [41] to make the high-level feature representations of the downstream classifiers between the restored image \mathbf{x}_r and the clean image \mathbf{x} close to each other. Specifically, we compute the ℓ_2 distance between their feature representations at each layer weighted by a layer-wise hyperparameter as

$$d(\mathbf{x}_r, \mathbf{x}) = \sum_l \frac{1}{H_l W_l} \sum_{h,w} \|w_l \odot (\hat{y}_{rhw}^l - \hat{y}_{chw}^l)\|_2^2, \quad (5)$$

where l denotes a certain layer in the network, $\hat{y}_r^l, \hat{y}_c^l \in \mathcal{R}^{H_l \times W_l \times C_l}$ are the unit-normalize results in the channel dimension, and vector $w^l \in \mathcal{R}^{C_l}$ is used for scaling activation channels.

By summing up the aforementioned three losses, we have the overall loss L_{PT} for prompt tuning as

$$L_{PT} = L_{CE}(\mathbf{M}, \hat{\mathbf{M}}) + L_1(\mathbf{x}_r, \mathbf{x}) + d(\mathbf{x}_r, \mathbf{x}). \quad (6)$$

We perform gradient descent to minimize L_{CE} w.r.t. prompt_L and prompt_R for prompt tuning. The design of continuous representations also enables thorough exploration in the embedding space.

Few-shot learning. During prompt-tuning, we utilize a minimal number of images for few-shot tuning. Specifically, DIFFender is tuned on a limited set of attacked images (8-shot in the experiments) from a single scenario and a specific attack method, but can learn optimal prompts that generalize well to other scenarios and attacks, which makes the tuning module effective and straightforward.

4. Experiments

4.1. Experimental settings.

Datasets and network architectures. We consider ImageNet [5] for evaluation and compare with eight state-of-the-art defense methods: Image smoothing-based defenses, including JPEG [8] and Spatial Smoothing [38]; Image completion-based defenses, such as DW [11], LGS [23]

and SAC [20]; Feature-level suppression defense FNC [40] and Jedi [31], a defense based on entropy and diffusion-based defense DiffPure [24]. For classifiers, we consider two advanced classifiers trained on ImageNet: CNN-based Inception-V3 [30] and Transformer-based Swin-S [30].

Adversarial attacks. We employ AdvP [2] and LaVAN [17], which randomly select patch positions and generate perturbations. We also employ GDPA [18], which optimizes the patch’s position and content to execute attacks, and RHDE [33], which utilizes realistic stickers and searches for their optimal positions to launch adversarial attacks. To adaptively attack the baseline based on pre-processing, we approximate gradients using the BPDA [1], which implies that the defense methods are white-box against the attack methods and set the number of iterations for the attacks to 100. For adapting the attack on DIFFender, we use an additional Straight-Through Estimator (STE) [39] during backpropagation through thresholding operations. Additionally, due to the randomness introduced by the diffusion processes, we use the Expectation over Transformation (EOT) + BPDA attack [1].

Evaluation metrics. We evaluate the performance of defenses under standard accuracy and robust accuracy. Due to the computational cost of adaptive attacks, unless otherwise specified, we assess the robust accuracy on a fixed subset of 512 sampled images from the test set. To facilitate the observation of changes, we ensure that the selected subset consists of images correctly classified.

4.2. Evaluation on ImageNet

Experimental results. Tab. 1 presents the experimental results, where the highest accuracy is highlighted in bold. Based on these results, we draw the following conclusions:

(1) DIFFender outperforms in defense effectiveness. Under adaptive attacks utilizing gradients, such as the BPDA+AdvP and BPDA+LaVAN, DIFFender exhibits superior performance, even only involving an 8-shot process. Other attacks like GDPA may not achieve strong attack effectiveness, but DIFFender still attains the highest robust accuracy. This can be attributed to that DIFFender is built upon the unified diffusion framework. Intuitively, the diffusion model can effectively remove adversarial areas while ensuring a high-quality and diverse generation that closely follows the underlying distribution of clean data. Additionally, the inherent stochasticity in the diffusion model allows for robust stochastic defense mechanisms [13], which makes it a well-suited “defender” for adversarial attacks.

(2) Image processing defense methods, such as JPEG, SS, and DW, experience a significant decrease in robust accuracy under adaptive attacks. This can be attributed to the algorithms’ gradients can be easily obtained. Other methods, such as LGS, FNC, SAC and Jedi, consider the robustness against adaptive attacks. For instance, FNC achieves

Table 1. Clean and robust accuracy against patch attacks on ImageNet by Inception-V3 and Swin-S.

Defense \ Attack	Inception-V3					Swin-S				
	Clean	AdvP	LaVAN	GDPA	RHDE	Clean	AdvP	LaVAN	GDPA	RHDE
Undefended	100.0	0.0	8.2	64.8	39.8	100.0	1.6	3.5	78.1	51.6
JPEG [8]	48.8	0.4	15.2	64.8	13.3	85.2	0.8	5.9	77.0	38.7
SS [38]	72.7	1.2	14.8	57.8	16.4	86.3	2.3	5.5	68.8	34.8
DW [11]	87.1	1.2	9.4	62.5	28.5	88.3	0.0	5.1	77.3	66.0
LGS [23]	87.9	55.5	50.4	67.2	49.6	89.8	65.6	59.8	82.0	69.1
FNC [40]	91.0	61.3	64.8	66.4	46.5	91.8	6.3	7.4	77.0	63.7
DiffPure [24]	65.2	10.5	15.2	67.6	44.9	74.6	18.4	26.2	77.7	62.3
SAC [20]	92.8	84.2	65.2	68.0	41.0	93.6	92.8	84.6	79.3	54.9
Jedi [31]	92.2	67.6	20.3	74.6	47.7	93.4	89.1	12.1	78.1	67.6
DIFFender	91.4	88.3	71.9	75.0	53.5	93.8	94.5	85.9	82.4	70.3

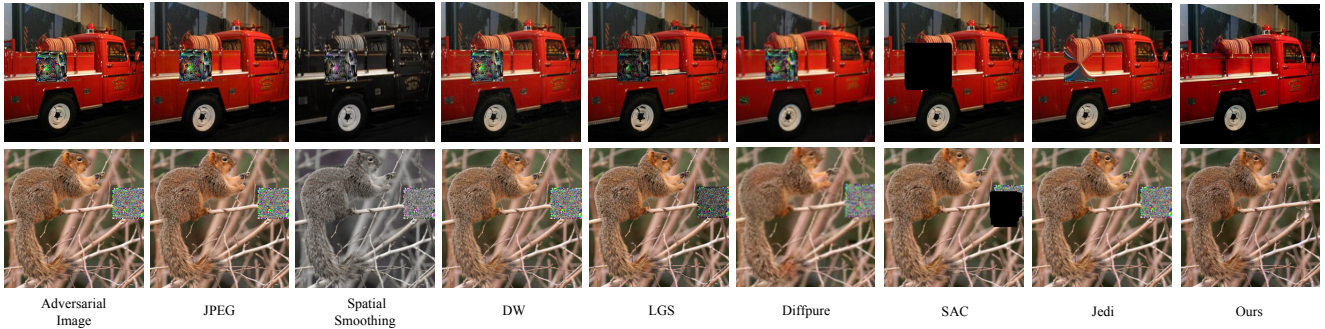


Figure 6. Visualization with examples from ImageNet. The restored images of DIFFender no longer show any traces of the patch, and the restored details are remarkable (e.g., the recovery of tree branches in the second column of images).

respectable robust accuracy on Inception-v3. However, its defense effectiveness diminishes when applied to the Swin-S. This is because the feature norm clipping layer proposed is specifically designed for handling CNN feature maps, while DIFFender exhibits excellent generalization capabilities that can extend to different classifiers.

(3) In the experiments, DIFFender only undergoes 8-shot prompt-tuning specifically for the AdvP method. This demonstrates the generalization capability of DIFFender to handle unseen attack methods. For Jedi, it has strong robustness against several attack methods, such as AdvP, but its robust accuracy has significantly decreased under other methods, like LaVAN. This might be because the autoencoder used by Jedi is trained under a specific style and cannot generalize well.

(4) When defending against global perturbations with ℓ_p -norm constraints, DiffPure achieves excellent results. However, it performs poorly when facing patch attacks. Specifically, in Tab. 1, when tested against AdvP and LaVAN, the inception-v3 model purified by DiffPure only maintains robust accuracy rates of 10.5% and 15.2%, respectively. This is also consistent with our observations in Section 3.1

Visualization. Fig. 6 presents the defense results of the defense methods against patch attacks. Since FNC suppresses the feature maps during the inference stage, it is not shown

in Fig. 6. Other methods, such as JPEG and DW, only exhibit minor changes in the reconstructed images and fail to defend against adaptive attacks. After Spatial Smoothing defense, the images show color distortion and are still vulnerable to attacks. In the case of the LGS method, the patch area is visibly suppressed, which improves the robust accuracy to some extent, but the patch is not completely eliminated. For Jedi and SAC, their localization algorithm fails under certain scenarios, as the second line in Fig. 6. And the restored results of Jedi cannot achieve complete recovery. On the other hand, the restored images of DIFFender no longer show any traces of the patch, and the restored details are remarkable.

4.3. Ablation studies and additional results

Table 2. Ablation study for different loss functions of DIFFender.

			Inception-V3				
L_{CE}	L_1	d	Clean	AdvP	LaVAN	GDPA	RHDE
✓	✓	✓	91.8	76.2	66.0	72.3	49.2
✓	✓	✓	88.3	87.1	69.5	73.8	52.7
✓	✓	✓	90.2	87.1	69.1	73.0	52.0
✓	✓	✓	91.4	88.3	71.9	75.0	53.5

Impact of loss functions. To evaluate the effectiveness of different losses, we conduct separate tuning experiments by

Table 3. Ablation study for different modules in DIFFender. DIFFender (NR) denotes “No Restoration”.

Defense	Inception-V3					Swin-S				
	Clean	AdvP	LaVAN	GDPA	RHDE	Clean	AdvP	LaVAN	GDPA	RHDE
DIFFender (NR)	86.3	84.0	66.8	69.5	48.0	88.7	92.2	81.8	78.9	69.1
DIFFender	91.4	88.3	71.9	75.0	53.5	93.8	94.5	85.9	82.4	70.3

Table 4. Ablation study for different prompt forms. “EP” and “MP” represent “Empty Prompt” and “Manual Prompt”.

Defense	Inception-V3					Swin-S				
	Clean	AdvP	LaVAN	GDPA	RHDE	Clean	AdvP	LaVAN	GDPA	RHDE
DIFFender (EP)	89.1	76.4	66.8	71.1	47.0	93.2	89.8	81.4	79.3	65.7
DIFFender (MP)	87.3	77.9	68.2	70.3	47.8	92.2	91.2	82.4	77.0	67.6
DIFFender	91.4	88.3	71.9	75.0	53.5	93.8	94.5	85.9	82.4	70.3

Table 5. DIFFender transferability performance on ResNet50 and ViT-B-16 for ImageNet.

Defense	ResNet-50					ViT-base				
	Clean	AdvP	LaVAN	GDPA	RHDE	Clean	AdvP	LaVAN	GDPA	RHDE
Undefended	100.0	0.0	14.8	73.8	37.1	100.0	1.2	2.0	76.2	52.0
DIFFender	83.6	83.2	55.9	76.2	53.5	91.0	88.3	85.2	78.9	68.0

removing loss functions L_{CE} , L_1 , and d separately, as presented in Tab. 2, where we observe that the robust accuracy significantly decreases when optimizing only the Restoration module without optimizing L_{CE} due to the performance loss in the localization, although it led to an improvement in clean accuracy. On the other hand, removing L_1 results in a noticeable decrease in clean accuracy, as images cannot be well restored. Eliminating either the d or L_1 causes a slight drop in robust accuracy. Finally, DIFFender, which incorporates all three loss functions, achieves the highest robust accuracy, demonstrating the importance of joint optimization and close interaction between the two modules for the overall performance of DIFFender.

Impact of restoration module. To verify the necessity of restoration, we remove the patch restoration and set the value in the \mathbf{M} region to zero. Experimental results in Tab. 3 show that the inclusion of patch restoration ensures better DIFFender performance. This is because patches may occasionally obscure crucial areas of an image, resulting in a loss of semantic information. The Restoration step can address this issue by recovering lost semantics, aiding classifiers in overcoming challenging scenarios. Furthermore, longer diffusion steps introduce more randomness, which preserves accuracy against adaptive attacks. Consequently, we conclude that the patch restoration is indeed necessary.

Impact of Prompt Tuning. In Tab. 4 we compared the complete DIFFender with the “Empty prompt” and “Manual prompt” versions of DIFFender. For DIFFender with manual prompts, we set $prompt_L$ = “adversarial” and $prompt_R$ = “clean”. The prompt-tuned DIFFender shows a significant improvement in robust accuracy compared to the other two zero-shot DIFFenders. This improvement, de-

spite exposure to only a few attacked images, underscores the effectiveness of prompt tuning.

Cross-model transferability. Specifically, we conduct 8-shot prompt-tuning on Inception-V3 and Swin-S. We then test the transferability of learned prompts on CNN-based ResNet50 [12] and transformer-based ViT-B-16 [7]. The results are presented in Tab. 5. DIFFender keeps high robust accuracy when applied to new classifiers. This demonstrates the good generalization capabilities of DIFFender.

4.4. Extension in Face Recognition.

Experimental settings. Facial expressions in human faces introduce a rich diversity, together with external factors such as lighting conditions and viewing angles, making face recognition a challenging task. We conducted experiments on the LFW [15], and employed two adversarial patch attacks: RHDE [33] and GDPA [18] mentioned above.

Table 6. Clean and robust accuracy against patch attacks on LFW.

Defense	FaceNet		
	Clean	GDPA	RHDE
Undefended	100.0	56.3	42.8
JPEG [8]	44.1	16.8	17.8
SS [38]	19.9	8.2	3.5
DW [11]	37.1	15.2	7.2
LGS [23]	60.9	71.9	53.5
FNC [40]	100.0	39.8	39.3
SAC [20]	100.0	77.3	43.2
Jedi [31]	100.0	74.2	43.9
DIFFender (EP)	100.0	79.3	57.2
DIFFender (MP)	100.0	77.0	57.2
DIFFender	100.0	81.1	60.7

Experimental results. The results on the LFW dataset are



Figure 7. DIFFender defense demonstrations against meaningless and meaningful patch attacks in the physical world. Noticing the mask edges may extend slightly beyond the patch region, aids in restoring the patch and helps maintain consistency in the restored image.

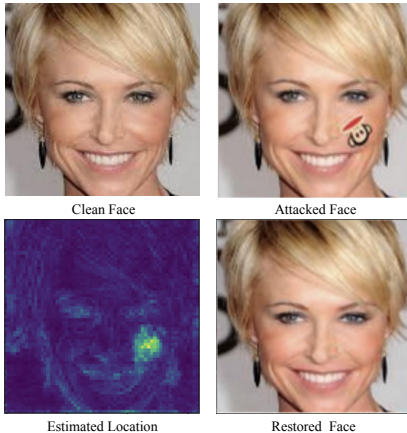


Figure 8. Visualization with examples from LFW attacked by RHDE, localized and restored by DIFFender.

presented in Tab. 6. DIFFender achieves the highest robust accuracy under both the GDPA and RHDE while ensuring clean accuracy. It is worth noting that DIFFender is not re-tuned specifically for facial recognition. This further demonstrates the generalizability of DIFFender across different scenarios and attack methods. In contrast, JPEG, SS, and the FNC method obtained low robust accuracies, even below the clean accuracy. This is because in the specific context of facial recognition, the classifier focuses more on crucial local features, and preprocessing the entire image can disrupt these important features. Fig. 8 illustrates the results of DIFFender against face attacks. It can be observed that DIFFender accurately identifies the location of the patch and achieves excellent restoration.

4.5. Extension in Physical World.

We additionally conduct further experiments in the physical world, where select 10 common object categories from

Table 7. Quantitative accuracy of meaningless physical attacks on the Inception-v3 at different angles and distances, along with the quantized results after defense by DIFFender.

	0°	yaw $\pm 15^\circ$	yaw $\pm 30^\circ$	pitch $\pm 15^\circ$	distance
Undefended	28.9	34.8	41.8	36.7	35.9
DIFFender	80.9	76.6	77.7	75.4	73.8

ImageNet and perform two types of patch attacks (meaningful and meaningless) [34]. Our approach involves generating digital-world attack results first, then placing stickers on real-world objects in the same positions. We test DIFFender under various conditions, including different angles (rotations) and distances. Qualitative results are depicted in Fig. 7, and additional results can be found in Appendix A.5, while quantitative results are presented in Tab. 7, where each configuration is based on 256 frames successfully classified images from the 10 objects selected. Based on the results, we see that DIFFender manifests substantial defensive capabilities across various physical alterations, maintaining its efficacy in real-world scenarios.

5. Discussion and Conclusion

We propose **DIFFender**, a novel defense method that leverages a pre-trained unified diffusion model to perform both localization and restoration of patch attacks. Additionally, we design a few-shot prompt-tuning algorithm to facilitate simple and efficient tuning. To show the robust performance of our method, we conduct experiments on image classification, further validate our approach on face recognition and finally extend to the physical world. Our research findings demonstrate that DIFFender exhibits superior robustness even under adaptive attacks and extends the generalization capability of pre-trained large models to various scenarios, diverse classifiers, and multiple attack methods, requiring only a few-shot prompt-tuning. We

prove that DIFFender significantly reduces the success rate of patch attacks while producing realistic restored images.

References

- [1] Anish Athalye, Nicholas Carlini, and David Wagner. Obfuscated gradients give a false sense of security: Circumventing defenses to adversarial examples. In *International conference on machine learning*, pages 274–283. PMLR, 2018. 1, 2, 5
- [2] Tom B Brown, Dandelion Mané, Aurko Roy, Martín Abadi, and Justin Gilmer. Adversarial patch. *arXiv preprint arXiv:1712.09665*, 2017. 1, 2, 5
- [3] Nicholas Carlini and David Wagner. Towards evaluating the robustness of neural networks. In *IEEE Symposium on Security and Privacy*, 2017. 1
- [4] Ping-yeh Chiang, Renkun Ni, Ahmed Abdelkader, Chen Zhu, Christoph Studer, and Tom Goldstein. Certified defenses for adversarial patches. *arXiv preprint arXiv:2003.06693*, 2020. 1, 2
- [5] Jia Deng, Wei Dong, Richard Socher, Li-Jia Li, Kai Li, and Li Fei-Fei. Imagenet: A large-scale hierarchical image database. In *2009 IEEE conference on computer vision and pattern recognition*, pages 248–255. Ieee, 2009. 5
- [6] Yinpeng Dong, Fangzhou Liao, Tianyu Pang, Hang Su, Jun Zhu, Xiaolin Hu, and Jianguo Li. Boosting adversarial attacks with momentum. In *Proceedings of the IEEE conference on computer vision and pattern recognition*, pages 9185–9193, 2018. 1, 2
- [7] Alexey Dosovitskiy, Lucas Beyer, Alexander Kolesnikov, Dirk Weissenborn, Xiaohua Zhai, Thomas Unterthiner, Mostafa Dehghani, Matthias Minderer, Georg Heigold, Sylvain Gelly, et al. An image is worth 16x16 words: Transformers for image recognition at scale. *arXiv preprint arXiv:2010.11929*, 2020. 7
- [8] Gintare Karolina Dziugaite, Zoubin Ghahramani, and Daniel M Roy. A study of the effect of jpg compression on adversarial images. *arXiv preprint arXiv:1608.00853*, 2016. 5, 6, 7
- [9] Ian J Goodfellow, Jonathon Shlens, and Christian Szegedy. Explaining and harnessing adversarial examples. *arXiv preprint arXiv:1412.6572*, 2014. 1, 2
- [10] Sven Gowal, Krishnamurthy Dj Dvijotham, Robert Stanforth, Rudy Bunel, Chongli Qin, Jonathan Uesato, Relja Arandjelovic, Timothy Mann, and Pushmeet Kohli. Scalable verified training for provably robust image classification. In *Proceedings of the IEEE/CVF International Conference on Computer Vision*, pages 4842–4851, 2019. 1, 2
- [11] Jamie Hayes. On visible adversarial perturbations & digital watermarking. In *Proceedings of the IEEE Conference on Computer Vision and Pattern Recognition Workshops*, pages 1597–1604, 2018. 1, 2, 5, 6, 7
- [12] Kaiming He, Xiangyu Zhang, Shaoqing Ren, and Jian Sun. Deep residual learning for image recognition. In *Proceedings of the IEEE conference on computer vision and pattern recognition*, pages 770–778, 2016. 7
- [13] Zhezhi He, Adnan Siraj Rakin, and Deliang Fan. Parametric noise injection: Trainable randomness to improve deep neural network robustness against adversarial attack. In *Proceedings of the IEEE/CVF Conference on Computer Vision and Pattern Recognition*, pages 588–597, 2019. 5
- [14] Jonathan Ho, Ajay Jain, and Pieter Abbeel. Denoising diffusion probabilistic models. *Advances in Neural Information Processing Systems*, 33:6840–6851, 2020. 1
- [15] Gary B Huang, Marwan Mattar, Tamara Berg, and Eric Learned-Miller. Labeled faces in the wild: A database for studying face recognition in unconstrained environments. In *Workshop on faces in 'Real-Life' Images: detection, alignment, and recognition*, 2008. 7
- [16] Pengfei Jing, Qiyi Tang, Yuefeng Du, Lei Xue, Xiapu Luo, Ting Wang, Sen Nie, and Shi Wu. Too good to be safe: Tricking lane detection in autonomous driving with crafted perturbations. In *Proceedings of USENIX Security Symposium*, 2021. 1
- [17] Danny Karmon, Daniel Zoran, and Yoav Goldberg. Lavan: Localized and visible adversarial noise. In *International Conference on Machine Learning*, pages 2507–2515. PMLR, 2018. 1, 2, 5
- [18] Xiang Li and Shihao Ji. Generative dynamic patch attack. *arXiv preprint arXiv:2111.04266*, 2021. 1, 2, 5, 7
- [19] Fangzhou Liao, Ming Liang, Yinpeng Dong, Tianyu Pang, Xiaolin Hu, and Jun Zhu. Defense against adversarial attacks using high-level representation guided denoiser. In *Proceedings of the IEEE conference on computer vision and pattern recognition*, pages 1778–1787, 2018. 5
- [20] Jiang Liu, Alexander Levine, Chun Pong Lau, Rama Chellappa, and Soheil Feizi. Segment and complete: Defending object detectors against adversarial patch attacks with robust patch detection. In *Proceedings of the IEEE/CVF Conference on Computer Vision and Pattern Recognition*, pages 14973–14982, 2022. 1, 5, 6, 7
- [21] Aleksander Madry, Aleksandar Makelov, Ludwig Schmidt, Dimitris Tsipras, and Adrian Vladu. Towards deep learning models resistant to adversarial attacks. *arXiv preprint arXiv:1706.06083*, 2017. 1, 2
- [22] Seyed-Mohsen Moosavi-Dezfooli, Alhussein Fawzi, and Pascal Frossard. Deepfool: a simple and accurate method to fool deep neural networks. In *Proceedings of the IEEE conference on computer vision and pattern recognition*, pages 2574–2582, 2016. 2
- [23] Muzammal Naseer, Salman Khan, and Fatih Porikli. Local gradients smoothing: Defense against localized adversarial attacks. In *2019 IEEE Winter Conference on Applications of Computer Vision (WACV)*, pages 1300–1307. IEEE, 2019. 1, 2, 5, 6, 7
- [24] Weili Nie, Brandon Guo, Yujia Huang, Chaowei Xiao, Arash Vahdat, and Anima Anandkumar. Diffusion models for adversarial purification. *arXiv preprint arXiv:2205.07460*, 2022. 1, 2, 5, 6
- [25] Sukrut Rao, David Stutz, and Bernt Schiele. Adversarial training against location-optimized adversarial patches. In *European Conference on Computer Vision*, pages 429–448. Springer, 2020. 1, 2

- [26] Robin Rombach, Andreas Blattmann, Dominik Lorenz, Patrick Esser, and Björn Ommer. High-resolution image synthesis with latent diffusion models. In *Proceedings of the IEEE/CVF Conference on Computer Vision and Pattern Recognition (CVPR)*, pages 10684–10695, 2022. 4
- [27] Mahmood Sharif, Sruti Bhagavatula, Lujo Bauer, and Michael K. Reiter. Accessorize to a crime: Real and stealthy attacks on state-of-the-art face recognition. In *ACM Sigsac Conference on Computer and Communications Security*, pages 1528–1540, 2016. 1
- [28] Jascha Sohl-Dickstein, Eric Weiss, Niru Maheswaranathan, and Surya Ganguli. Deep unsupervised learning using nonequilibrium thermodynamics. In *International Conference on Machine Learning*, pages 2256–2265, 2015. 1
- [29] Christian Szegedy, Wojciech Zaremba, Ilya Sutskever, Joan Bruna, Dumitru Erhan, Ian Goodfellow, and Rob Fergus. Intriguing properties of neural networks. *arXiv preprint arXiv:1312.6199*, 2013. 1
- [30] Christian Szegedy, Vincent Vanhoucke, Sergey Ioffe, Jon Shlens, and Zbigniew Wojna. Rethinking the inception architecture for computer vision. In *Proceedings of the IEEE conference on computer vision and pattern recognition*, pages 2818–2826, 2016. 5
- [31] Bilel Tarchoun, Anouar Ben Khalifa, Mohamed Ali Mahjoub, Nael Abu-Ghazaleh, and Ihsen Alouani. Jedi: Entropy-based localization and removal of adversarial patches. In *Proceedings of the IEEE/CVF Conference on Computer Vision and Pattern Recognition*, pages 4087–4095, 2023. 2, 5, 6, 7
- [32] Jinyi Wang, Zhaoyang Lyu, Dahua Lin, Bo Dai, and Hongfei Fu. Guided diffusion model for adversarial purification. *arXiv preprint arXiv:2205.14969*, 2022. 1, 2
- [33] Xingxing Wei, Ying Guo, and Jie Yu. Adversarial sticker: A stealthy attack method in the physical world. *IEEE Transactions on Pattern Analysis and Machine Intelligence*, 2022. 1, 2, 5, 7
- [34] Xingxing Wei, Bangzheng Pu, Jiefan Lu, and Baoyuan Wu. Physically adversarial attacks and defenses in computer vision: A survey. *arXiv preprint arXiv:2211.01671*, 2022. 8
- [35] Tong Wu, Liang Tong, and Yevgeniy Vorobeychik. Defending against physically realizable attacks on image classification. *arXiv preprint arXiv:1909.09552*, 2019. 1, 2
- [36] Chaowei Xiao, Zhongzhu Chen, Kun Jin, Jiong Xiao Wang, Weili Nie, Mingyan Liu, Anima Anandkumar, Bo Li, and Dawn Song. Densepure: Understanding diffusion models for adversarial robustness. In *The Eleventh International Conference on Learning Representations*, 2022. 1, 2
- [37] Zihao Xiao, Xianfeng Gao, Chilin Fu, Yinpeng Dong, Wei Gao, Xiaolu Zhang, Jun Zhou, and Jun Zhu. Improving transferability of adversarial patches on face recognition with generative models. In *Proceedings of the IEEE/CVF Conference on Computer Vision and Pattern Recognition*, pages 11845–11854, 2021. 1
- [38] Weilin Xu, David Evans, and Yanjun Qi. Feature squeezing: Detecting adversarial examples in deep neural networks. *arXiv preprint arXiv:1704.01155*, 2017. 5, 6, 7
- [39] Penghang Yin, Jiancheng Lyu, Shuai Zhang, Stanley Osher, Yingyong Qi, and Jack Xin. Understanding straight-through estimator in training activation quantized neural nets. *arXiv preprint arXiv:1903.05662*, 2019. 5
- [40] Cheng Yu, Jiansheng Chen, Youze Xue, Yuyang Liu, Weitao Wan, Jiayu Bao, and Huimin Ma. Defending against universal adversarial patches by clipping feature norms. In *Proceedings of the IEEE/CVF International Conference on Computer Vision*, pages 16434–16442, 2021. 1, 2, 5, 6, 7
- [41] Richard Zhang, Phillip Isola, Alexei A Efros, Eli Shechtman, and Oliver Wang. The unreasonable effectiveness of deep features as a perceptual metric. In *Proceedings of the IEEE conference on computer vision and pattern recognition*, pages 586–595, 2018. 5
- [42] Yiqi Zhong, Xianming Liu, Deming Zhai, Junjun Jiang, and Xiangyang Ji. Shadows can be dangerous: Stealthy and effective physical-world adversarial attack by natural phenomenon. In *Proceedings of the IEEE/CVF Conference on Computer Vision and Pattern Recognition*, pages 15345–15354, 2022. 2
- [43] Kaiyang Zhou, Jingkang Yang, Chen Change Loy, and Ziwei Liu. Learning to prompt for vision-language models. *International Journal of Computer Vision*, 130(9):2337–2348, 2022. 4
- [44] Zijian Zhu, Yichi Zhang, Hai Chen, Yinpeng Dong, Shu Zhao, Wenbo Ding, Jiachen Zhong, and Shibao Zheng. Understanding the robustness of 3d object detection with bird’s-eye-view representations in autonomous driving. *arXiv preprint arXiv:2303.17297*, 2023. 1